A Comparison of Cellular Lattice Structures with Curved and Straight Inclined Walls

Matthew DiPalma,[1] and Farhan Gandhi[2]
Center for Mobility with Vertical Lift (MOVE)
Rensselaer Polytechnic Institute, Troy, NY, 12180

This paper compares hexagonal cellular lattice structures with straight and curved inclined walls, with cell angles varying between 15-60 deg, and wall thickness ratios between 5-20%. For loading in the y-direction, curved inclined walls exhibited in a higher modulus, with the largest increases at the highest cell angles examined (60 deg). Conversely, for loading in the x-direction, curved inclined walls exhibit a lower modulus with the greatest decreases at the lowest cell angles examined (15 deg). The predicted differences in stiffness between cells with straight and curved inclined walls is experimentally demonstrated. The increase in y-modulus as well as the reduction in x-modulus with the curved inclined walls is attributed to the lower wall slope at the wall junctions. The peak von-Mises stress at the junctions is generally lower for curved wall cells than for straight wall cells. The reduction exceeds 25% for loading both in the x-direction and y-direction.

Nomenclature

a	=	vertical to inclined wall length ratio
β	=	thickness ratio
δ_0	=	translation degree of freedom
η	=	vertical to inclined wall thickness ratio
θ	=	cell angle
θ_0	=	rotational degree of freedom
E	=	Young's modulus
I	=	second moment of area
L	=	inclined wall length
M_0	=	applied moment
P_0	=	applied force
x	=	horizontal direction
y	=	vertical direction

Introduction

Due to their high stiffness to weight ratio and considerable design flexibility, there is significant interest in the use of cellular lattice structures in a wide variety of structural applications. In their seminal work, Gibson and Ashby **(Ref. 1)** present the *Cellular Material Theory*, which provides expressions for global lattice properties (such as moduli in various directions) as a function of unit cell geometric parameters for traditional hexagonal lattices. Amongst various researchers who have used *Cellular Material Theory* as a point of departure to develop cellular lattice structures for a range of applications, Gandhi and co-workers have considered optimally designed lattices for morphing **(Refs. 2-6)**, lattices with inclusions in the unit cell to elicit specific behaviors **(Refs. 7-9)**, lattices with elastomeric infills to simultaneously meet stiffness and damping requirements **(Refs. 10-13)**, and responses of lattice structures to damage **(Ref. 14)**. ***However, in almost all of these studies, the hexagonal unit cells that constitute the building-blocks have straight (non-curved) walls.***

[1] Ph.D Student, NDSEG Fellow
[2] Rosalind and John J. Redfern Jr. '33 Professor of Aerospace Engineering, AIAA Associate Fellow

The walls of plant cells are composed of highly ordered crystalline sugar polymer aggregates called cellulose microfibrils which have a tensile strength comparable to steel and a significant elastic modulus (~130 GPa) **(Ref. 15)**, which allows plants to withstand large internal pressures (due to volume change) and external loadings (due to environmental forces) with great strength and resiliency. While the highly structured and ordered lattice formed by the relatively stiff walls of plant cells may take many forms (gridded rectangular lattice, standard hexagonal lattice, among others), many plant cells arrange themselves in a formation reminiscent of a hexagonal lattice but with curved inclined walls, as shown in the characteristic rigid Elodea leaf micrographed in **Figure 1**. It is therefore of some biologically-inspired interest to investigate the potential advantages of such curved-wall cellular lattice structures, when compared against traditional straight-walled hexagonal honeycombs.

The focus of the present study is to compare the behavior of hexagonal lattice structures with straight and curved inclined walls using finite element analyses. The effects of the inclined wall geometry on the global stiffnesses and peak stresses at the junctions of the cellular lattices are presented for a wide domain of parameters that characterize the overall lattice geometry. Analysis is conducted of lattices under loading in both the horizontal (x) and vertical (y) directions. Corresponding explanations of the structural mechanics that govern the differences between straight- and curved-wall lattices is also presented.

Analysis

Cellular lattices of tessellated unit cells are considered in this study, where the generic unit cell geometry is defined by a number of non-dimensional parameters, following **Ref. 1**. With some adaptation, this parametrization scheme can be applied to both traditional hexagonal honeycombs as well as the modified curved-wall lattices. As shown in **Figure 2**, θ represents the cell angle (relative to the horizontal, or x-axis), and β represents the thickness to length (slenderness) ratio of the inclined wall. Because this study compares the performance of various inclined wall geometries, the vertical to inclined wall length ratio parameter, α, is set to constant a value of unity. In *Cellular Material Theory*, the parameter, η, represents the vertical to inclined wall thickness ratio, but this parameter is also assigned a constant value of unity in the current study. The inclined wall "net" length, L, is taken to be 20 mm in this study, but in *Cellular Material Theory* the lattice properties are understood to be independent of wall length. The depth of the structure is not relevant to the results presented, but is taken to be ¼ inch, which is a common nominal thickness for plastics and metals that can be waterjet cut for experimental validation. The material of interest in this study is Aluminum.

The shape of the curved walls can then be characterized in terms of these parameters by a simple sinusoid as follows:

$$y = \pm \frac{L \sin(\theta)}{2} \cos\left(\frac{\pi x}{L \cos(\theta)}\right)$$

where y is the vertical coordinate and x is the horizontal coordinate measured from the point at which the vertical wall joins with the inclined walls. Naturally, the arc length of the curved inclined wall is longer than that of the straight inclined wall, which lends itself to lattices of the curved cells having a higher volume and mass than the traditional honeycomb lattices.

One of the very attractive features of cellular lattice structures is that full-lattice behavior can be predicted based on the analysis/behavior of a properly constrained single unit cell, which greatly reduces the computational expense. In ABAQUS 6.13, C3D20R brick elements are used to model single lattice cells, with 6-7 mesh elements through the wall thickness and 25-30 elements along the wall length. Such mesh fidelity has been shown to produce converged results in **Refs. 10-13**. An arbitrary unit cell is represented by a mesh of around 40,000 elements, which corresponds to around 600,000 degrees of freedom, depending on the specific cell geometry. An example of the mesh is shown in **Figure 3** (β=0.1, θ=45 deg).

Straightforward boundary conditions that enforce the lattice effect are implemented and shown in **Figure 4**: vertical walls remain vertical, and regions opposite the applied loading are simulated to be on rollers. Geometric nonlinearity is considered in this study, but material nonlinearities are neglected.

In most applications, the stiffness of a lattice is one of the most important measures of its performance. A lattice with great stiffness deforms less under certain loading than a lattice of less stiffness. In aerospace applications, honeycomb lattices are often selected which provide threshold structural stiffnesses at minimum weight. As such, it is of interest to determine the relative difference between the stiffness of lattices with curved and straight inclined walls. To that effect, results from a parametric sweep of the 3D finite element analysis is presented below. Cell angle, θ, varies from 15-60 deg and thickness ratio, β, varies from 5-20%.

Results

Figure 5 depicts the system modulus for various cell geometries under y-direction loading. As expected, cells with high values of β and high values of θ are the stiffest for lattices with both straight and curved inclined walls. Throughout the entire design space, lattices with curved inclined walls are observed to have greater stiffness than lattices with straight inclined walls. **Figure 6 (left)** presents ratios of y-moduli of curved to straight inclined wall lattices. Based on the scale on **Fig. 6 (left)**, it is evident that the cells with curved inclined walls always have a lower y-modulus than corresponding cells with straight inclined walls. The maximum stiffness ratio of curved to straight inclined wall cells is observed to be 1.88 for high cell angles (θ=60 deg) and low wall thickness (β=5%). The absolute difference between y-moduli of curved and straight inclined wall cells is shown in **Fig. 6 (right)**. The greatest absolute difference is 220 ksi, which is again at the highest cell angles (θ=60 deg) but at higher wall thickness values (β=20%).

Because lattices with curved inclined walls have a higher frontal area than lattices with straight inclined walls, their weight is also greater. **Figure 7** illustrates the relative increase in frontal area for the lattice with curved inclined walls over the lattice with straight inclined walls. For any given combination of geometric parameters, a typical lattice with curved inclined walls is less than 4% heavier than the corresponding lattice with straight inclined walls.

The system modulus for various cell geometries under x-direction loading is shown in **Figure 8**. As expected, cells with high values of β and low values of θ are the stiffest for lattices with both straight and curved inclined walls. In this orientation, the lattices with straight inclined walls have a moderate stiffness advantage over the lattices with curved inclined walls. **Figure 9 (left)** presents ratios of x-moduli of curved to straight inclined wall lattices. For low-to-moderate cell angles, the lattices with curved inclined walls are more compliant than their straight walled counterparts. In particular, the curved-wall geometry with β=0.05 and θ=15 deg is 37% more complaint than the straight walled geometry. The absolute difference between x-moduli of curved and straight inclined wall cells is shown in **Fig. 9 (right).** For low values of β and high values of θ, the cells with straight inclined walls have the greatest difference in stiffness. For example, the straight-wall geometry with β=0.05 and θ=60 deg is 193 ksi stiffer than the curved-wall geometry.

Another major difference between lattices with curved inclined walls and lattices with straight inclined walls are the angles that the walls make at the junctions. Referring to the geometries in **Figure 10**, the interior angles of the curved-wall cell shown amount to four 90 deg angles and two 180 deg angles, whereas the interior angles of the straight-wall cell shown amount to four (90+θ) deg angles and two (180-2θ) deg angles.

Figure 11a illustrates the von Mises stress on the surface of two cells (β=0.125, θ=45 deg) loaded extensionally with 1 ksi in the x-direction. At the junction marked B on these cells, the peak stress is 25%

lower for the curved wall cell than observed for the cell with the straight inclined walls. A similar trend is visible under a 1 ksi loading in the y-direction in **Figure 11b**, in which the curved lattice experiences a 26% reduction in peak von Mises stress. In the absence of fileting and other corner-smoothing techniques, a lattice of moderate (45 deg) cell angle with curved inclined walls experiences lower peak stresses making it less susceptible crack propagation and fatigue failure than an otherwise identical lattice with straight inclined walls.

Figure 12 depicts the peak von Mises stress ratio between lattices with curved and straight inclined walls across the design space under equal loading in the x-direction. Ratios below 1 indicate geometries for which the peak stress is lower for curved-wall lattices than for straight-wall lattices. Lattices with curved inclined walls exhibit lower peak stresses under x-direction loading, with reductions exceeding 25%. **Figure 13** depicts the peak von Mises stress ratio for loading in the y-direction. Again, lattices with curved inclined walls exhibit lower stiffness-normalized peak stresses, up to a maximum exceeding 25%. This trend does not apply to lattice geometries with very shallow cell angles (θ=15 deg), where the stiffness-normalized peak von Mises stress ratio exceeds 1.

When loaded in the y-direction, straight-walled cells exhibit the highest von Mises stresses at the junctions marked B, and the absolute von Mises stress at all junctions decreases with increasing cell angle. However, for curved-walled cells the peak von Mises stress appears at junction A for shallow cell angles and junction B for steep cell angles. For these curved wall cells, the stresses at both junctions also decreases with cell angle, but the stress at junction A decreases more rapidly, which causes the shift in the region at which the cell's peak stress occurs. The switch in location of peak stress can be observed by comparing the curved-wall cells in **Figure 11b** (θ=45 deg), where the peak is at junction B, and **Figure 14** (θ=15 deg), where the peak is at junction A. Referring to the same figures, the location of peak stress does not change in straight walled cells, with the peak always at junction B.

Another difference between the vertices of lattices with curved inclined walls and lattices with straight inclined walls is that curved-wall lattices have constant interior angles regardless of cell angle. On the other hand, a straight-walled lattice has interior angles that vary with cell angle. The constancy of interior angles for curved-wall lattices might lend itself to a simplified system for both modeling and manufacture.

Figure 15 shows a couple of test articles (β=0.2, θ=30 deg) which have been waterjet cut from ¼-inch aluminum for the purpose of experimental validation under tensile load. There are 2 specimens of each sample – with both straight and curved inclined walls. The large rectangular regions on the top and bottom of the sample serve as clamp locations for the tensile test machine. Additionally, under vertical loading the very large thickness of the left and right vertical cell walls inhibits bending deformation in these walls (something that would be suppressed in a large honeycomb by the presence of adjacent cells, but needs to be suppressed in a single cell test).

The load versus displacement results from a y-direction tensile test are presented in **Figure 16**. The cell with curved inclined walls is notably stiffer than its straight-walled counterpart across all trials; this confirms the conclusions drawn from the 3D finite element analysis. More importantly, the corresponding data points from the 3D finite element analysis fall along the load-displacement curve for both geometries, which adds confidence to the accuracy of the finite element results.

Why does this happen?

In order to understand the physical mechanisms behind the performance differences, a simplified analytical model based on Castigliano's energy method was developed and implemented. The inclined walls are modeled as slender beams undergoing pure bending, and this slenderness assumption holds true for

moderate values of β. The internal energy stored as bending along the path, s, of the inclined walls is expressed as:

$$U = \frac{1}{2EI}\int M(s)^2 ds \quad (1)$$

$$M(x) = M_0 + \frac{P_0}{2}\left(x - Lcos(\theta)\right) \quad (2)$$

where P_0 is the applied vertical load and M_0 is the boundary moment imposed to prevent rotation at the ends of the beam, as shown in **Figure 17**. The slopes of the straight and curved inclined walls are used to transform from the path variable, s, to the global coordinate, x:

$$ds = \sqrt{dx^2 + dy^2} = dx\sqrt{1 + \left(\frac{dy}{dx}\right)^2} \quad (3)$$

$$\frac{dy_{straight}}{dx} = \tan(\theta) \quad (4a)$$

$$\frac{dy_{curved}}{dx} = \frac{\pi \tan(\theta)}{2} sin\left(\frac{\pi x}{Lcos(\theta)}\right) \quad (4b)$$

The two degrees of freedom of relevance are the rotation and vertical displacement at the top of the beam. Using Castigliano's method we can express these quantities in terms of their corresponding energy derivatives:

$$\delta_0 = \frac{dU}{dP_0} = \frac{1}{2EI}\int \frac{dM(x)^2}{dP_0}\, dx\sqrt{1 + \left(\frac{dy}{dx}\right)^2} \quad (5a)$$

$$\theta_0 = \frac{dU}{dM_0} = \frac{1}{2EI}\int \frac{dM(x)^2}{dM_0}\, dx\sqrt{1 + \left(\frac{dy}{dx}\right)^2} \quad (5b)$$

Because P_0 is a known applied load and θ_0 is required to be zero for symmetry, **Equation 5b** (or simple statics) can be used to solve for M_0. Once M_0 is known, the vertical tip displacement δ_0 can be calculated for both the straight- and curved-wall cells per **Equation 5a**. The vertical tip displacements for the inclined walls for the quarter-cells can be extended to model the performance of the full cell. The vertical cell walls also undergo a small net extension under vertical load, which is also considered using basic Strengths of Materials.

This simple analytical model compares well against 2D finite beam element analysis of the cellular structures. **Figure 18** compares the applied load required to achieve 1% vertical strain for the straight- and curved-wall cells (θ=45 deg) for the two models. The vastly simplified analytical model closely matches the finite element model for low values of β, and it maintains less than 5% error for higher values of β, where the slenderness assumption becomes less valid.

Figure 19 depicts the bending energy distribution along the inclined wall for straight- and curved-wall cells under 1% strain in the y-direction (β=0.2, θ=45 deg). For this geometry, the y-modulus for the curved- wall cell is 18% greater than for the straight-walled cell. The curved-wall cell has more internal bending energy stored along the inclined wall length at a given strain level. This corresponds to a higher load requirement for the curved-wall cell and a correspondingly greater stiffness in the y-direction.

Figure 20 depicts the bending energy distribution along the inclined wall for the straight- and curved-wall cell but under a 10-pound load in the y-direction (β=0.2, θ=45 deg). While the bending energy is comparable between the two cells around the central region of the inclined wall, there is a significant difference at either end of the inclined wall. The straight-walled cell undergoes significantly more bending than its curved counterpart near the ends, which increases the compliance where the bending energy is greatest (and reduces the modulus of the cell).

Under the same applied y-load, the straight-wall cell undergoes more bending at either end because it has a higher slope at those locations. At the junctions, the straight-wall cells are inclined at the cell angle, θ, whereas the curved-wall cells have zero slope. The integrand in **Equations 1**, **5a**, and **5b** are all scaled by the coordinate transformation in **Equation 3**, which increases with the slope of the inclined wall. The bending moment diagram for the inclined wall is depicted in **Figure 21**. Because the magnitude of the sectional moment is greatest where the slope of the straight inclined walls is finite and the slope of the curved inclined walls is zero, this scaling in compliance is compounded. On the other hand, at the midpoint of the inclined wall where the curved walls have their highest slope, the sectional bending moment is zero. **In short, the curved inclined walls are more efficient in distributing their geometric bending stiffness because their shapes are innately stiff in regions of high sectional moment and innately compliant in regions of low sectional moment.**

Of course, this relative stiffness increase is highly orientation-dependent. While the curved inclined wall is advantageous under y-direction loading, it becomes disadvantageous under x-direction loading, as is evident in the previous set of results. This follows the previous physical explanation. Because the orientation changes, the zero slope of the curved inclined walls becomes a right angle in the reoriented system. In that orientation, the curved walls have a higher slope in regions of high applied moment and a low slope in regions of low applied moment. In effect, the same geometric features that produce stiffness advantage under y-direction loading produce a stiffness disadvantage in x-direction loading – for exactly the same reason.

This physical understanding of the mechanics can also be leveraged to understand fundamental trends in the design space. Consider lattices with fixed cell angle, θ, and varying wall thickness ratio, β. Because the bending energy and deflections (in **Equations 1**, **5a**, and **5b**) scale inversely with the second moment of area, I, these quantities should decrease with the cube of β – which can be qualitatively observed along lines of constant θ in **Figures 5** and **8**.

Consider the relative difference in lattice y-modulus presented in **Figure 6**. For a given β, the greatest relative difference between lattices with curved and straight inclined walls occurs at higher values of θ. Higher values of cell angle are associated with greater inclined wall slope. Such high inclined wall slopes drastically decrease the y-direction stiffness properties of the straight-wall lattices relative to the curved-wall lattices, per the preceding explanation. Curved wall lattices, on the other hand, are insulated from effects of large cell angle because they have zero slope in regions of maximum applied bending moment and large slopes in regions of low applied bending moment.

The same physical explanation can also be applied to this trend in the x-direction. Consider the relative difference in lattice y-modulus presented in **Figure 9**. For a given β, the greatest relative difference between lattices with curved and straight inclined walls occurs at lower values of θ. In particular, at θ=15 deg, curved wall lattices become 30-35% more compliant than their straight-walled counterparts. This is because low cell angles increase the net inclined wall slope in the rotated system. Such an increase in inclined wall slope affects the curved-wall lattices to a greater extent than the straight-walled lattices because the curved-wall lattices still have near-infinite slopes in regions of maximum applied bending moment and low slope in regions of low applied bending moment.

Summary and Concluding Remarks

This paper compares cellular lattice structures with (1) hexagonal cells with straight inclined walls, and (2) cells where the inclined walls are curved. The study uses ABAQUS Finite Element simulations, experimental verification, and analytical expressions to explain observed differences. Simulations covered variations in cell angle from 15-60 deg, and cell wall thickness ratio from 0.05-0.2. From the results presented, the following observations could be drawn:

1. For loading in the y-direction, when the inclined walls were curved the cells always had a higher modulus than cells with straight inclined walls, with the difference being greatest at the high (60 deg) cell angles. The curved to straight inclined wall y-modulus ratio is greatest at low (5%) wall thickness, but the absolute difference in stiffness is greatest at high (20%) wall thickness. At a cell angle of 60 deg, the y-modulus ratio varies between 1.26 (at 20% wall thickness) to 1.88 (at 5% wall thickness).
2. For loading in the x-direction, when the inclined walls were curved the cells generally had a lower modulus than cells with straight inclined walls, with the difference being greatest at the low (15 deg) cell angles. The curved to straight inclined wall x-modulus ratio is lowest at low (5%) wall thickness, but the absolute difference in stiffness is greatest at high (20%) wall thickness. At a cell angle of 15 deg, the x-modulus ratio (curved to straight inclined walls) varies between .63 (at 5% wall thickness) to 0.72 (at 20% wall thickness).
3. For the hexagonal cells with straight inclined walls, the interior angles at four junctions are (θ + 90) deg and those at the other two (top and bottom) junctions are ($180 - 2\theta$) deg. The corresponding interior junction angles in the case of the curved inclined walls approaches 90 deg and 180 deg. Under loading, the stiffness-normalized peak von-Mises stresses at the top and bottom junctions were reduced by over 25% in the case of the curved walls compared to the straight inclined walls under loading in both the x- and y-directions.
4. Straight wall cells experience peak von Mises stresses at the junction vertex at the top/bottom of each cell, regardless of cell angle. Curved wall cells experience peak von Mises stresses at the upper/lower junction vertices for steep cell angles and at the edge junction vertices for shallow cell angles. The overall von Mises stress values decrease with cell angle at all vertices.
5. For a 45 deg cell angle, 20% wall thickness cells, the differences in modulus predicted by the simulations compared well with the experimental results, for loading in both x- and y-directions.
6. For loading in the y-direction, higher values of cell angle increase the modulus. For curved walls, the horizontal stumps near the junctions are very stiff in bending, and the walls are effectively steeper away from the junctions which increases the y-modulus. Conversely, for loading in the x-direction, higher values of cell angle decrease the modulus. For curved walls, the horizontal stumps near the junctions do not undergo bending, and the walls are effectively steeper away from the junctions which decreases the x-modulus.

Acknowledgements

Matthew DiPalma is supported by the Department of Defense through the National Defense Science and Engineering Graduate (NDSEG) Fellowship Program.

References

1. Gibson, L. and Ashby, M., *Cellular Solids, Structure and Properties*, 2nd Edition, Cambridge University Press, Cambridge, 1999.
2. Olympio, K. R., and Gandhi, F., "Flexible Skins for Morphing Aircraft using Cellular Honeycomb Cores," *Journal of Intelligent Material Systems and Structures*, Vol. 21 (17), November 2010, pp. 1719-1735, doi:10.1177/1045389X09350331.

3. Olympio, K. R., and Gandhi, F., "Zero-Poisson's Ratio Cellular Honeycombs for Flexskins Undergoing One-Dimensional Morphing," *Journal of Intelligent Material Systems and Structures*, Vol. 21 (17), November 2010, pp. 1737-1753, doi:10.1177/1045389X09355664
4. Olympio, K. R., Gandhi, F., Asheghian, L., and Kudva, J., "Design of a Flexible Skin for a Shear Morphing Wing," *Journal of Intelligent Material Systems and Structures*, Vol. 21 (17), November 2010, pp. 1755-1770, doi:10.1177/1045389X10382586.
5. Olympio, K. R., and Gandhi, F., "Optimal Cellular Core Topologies for One-Dimensional Morphing Aircraft Structures," *J. Mech. Des*., Aug. 2012, 134(8), 081005, http://dx.doi.org/10.1115/1.4007087.
6. Barbarino, S., Gandhi, F., and Webster, S., "Design of Extendable Chord Sections for Morphing Helicopter Rotor Blades," *Journal of Intelligent Material Systems and Structures*, Vol. 22 (9), June 2011, pp. 891-905, doi: 10.1177/1045389X11414077.
7. Pontecorvo, M., Barbarino, S., and Gandhi, F., "Cellular Honeycomb-Like Structures with Internal Inclusions in the Unit-Cell," *Proceedings of the ASME 2012 Conference on Smart Materials, Adaptive Structures and Intelligent Systems, SMASIS2012*, Sept. 19-21, 2012, Stone Mountain, Georgia, SMASIS2012-8075.
8. Barbarino, S., Pontecorvo, M., and Gandhi, F., "Cellular Honeycomb-Like Structures with Internal Buckling and Viscous Elements for Simultaneous Load-Bearing and Dissipative Capability," *Proceedings of the ASME 2012 Conference on Smart Materials, Adaptive Structures and Intelligent Systems, SMASIS2012*, Sept. 19-21, 2012, Stone Mountain, Georgia, SMASIS2012-8080.
9. Pontecorvo, M., Niemiec, R., and Gandhi, F., "Design studies on cellular structures with pneumatic artificial muscle inclusions for modulus variation," *Journal of Intelligent Material Systems and Structures*, September 2015, DOI: 10.1177/1045389X15604404.
10. Murray, G., Gandhi, F., and Hayden, E., "Polymer Filled Honeycombs to Achieve a Structural Material with Appreciable Damping," *Journal of Intelligent Material Systems and Structures*, Vol. 23, No. 6, April 2012, pp. 703-718.
11. Murray, G., and Gandhi, F., "Auxetic Honeycombs with Lossy Polymeric Infills for High Damping Structural Materials," *Journal of Intelligent Material Systems and Structures*, Vol. 24, No. 9, June 2013, pp.1090-1104.
12. DiPalma, M. and Gandhi, F., "Cellular Lattices with an Internal Topology for High Stiffness and Damping", 57th AIAA/ASCE/AHS/ASC Structures, Structural Dynamics, and Materials Conference, AIAA SciTech, January 7, 2016.
13. DiPalma, M. and Gandhi, F., "Optimizing Stiffness and Damping of Filled Cellular Lattice Structures using Response Surface Methods", 58th AIAA/ASCE/AHS/ASC Structures, Structural Dynamics, and Materials Conference, AIAA SciTech, January 2017.
14. DiPalma, M. and Gandhi, F., " Stress Redistribution in Cellular Lattice Structures with Cell Wall Damage", 59th AIAA/ASCE/AHS/ASC Structures, Structural Dynamics, and Materials Conference, AIAA SciTech, January 2018.
15. Nishiyama, Yoshiharu. "Structure and properties of the cellulose microfibril." *Journal of Wood Science* 55.4 (2009): 241-249.

Figure 1 – Curved cell walls of Elodea leaf (water weed) under microscope

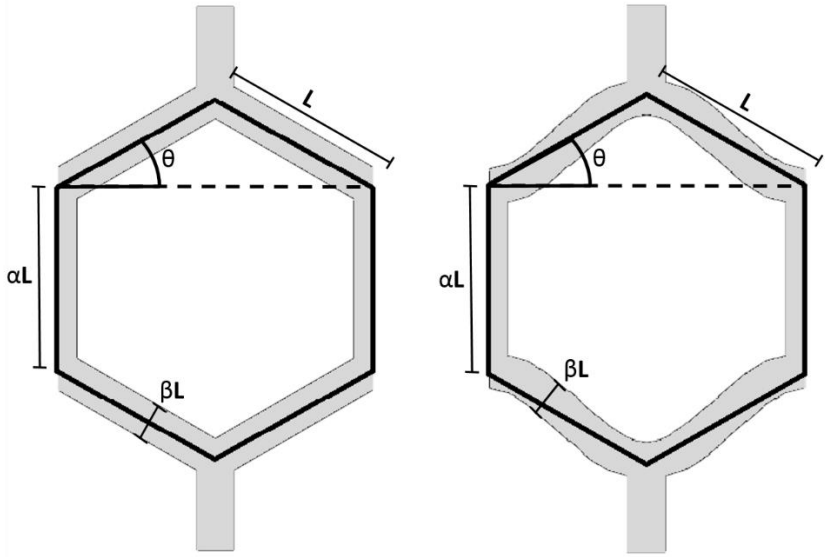

Figure 2 – Nondimensional parameters applied to straight- and curved-wall cellular lattices

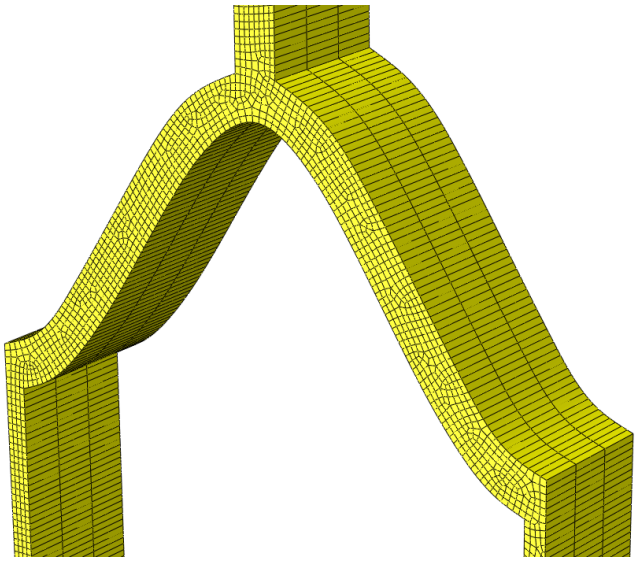

Figure 3 – Sample of 3D finite element mesh (β=0.1, θ=45 deg)

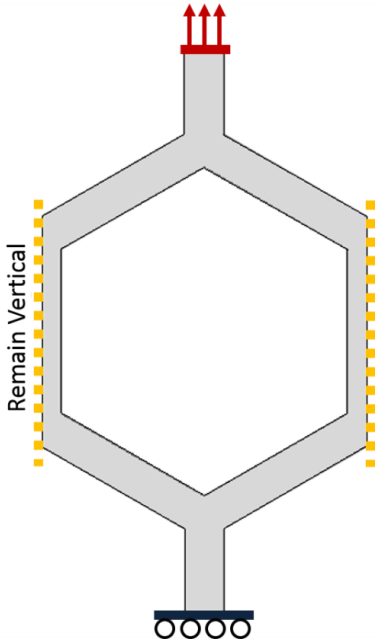

Figure 4 – Sample boundary conditions enforced on generic unit cell undergoing vertical extension

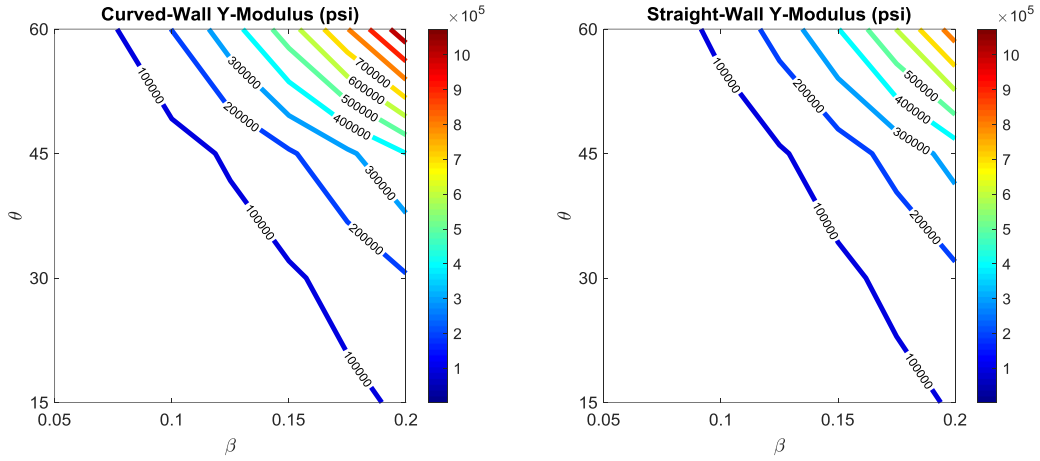

Figure 5 – System modulus (psi) for various cell geometries under y-direction loading

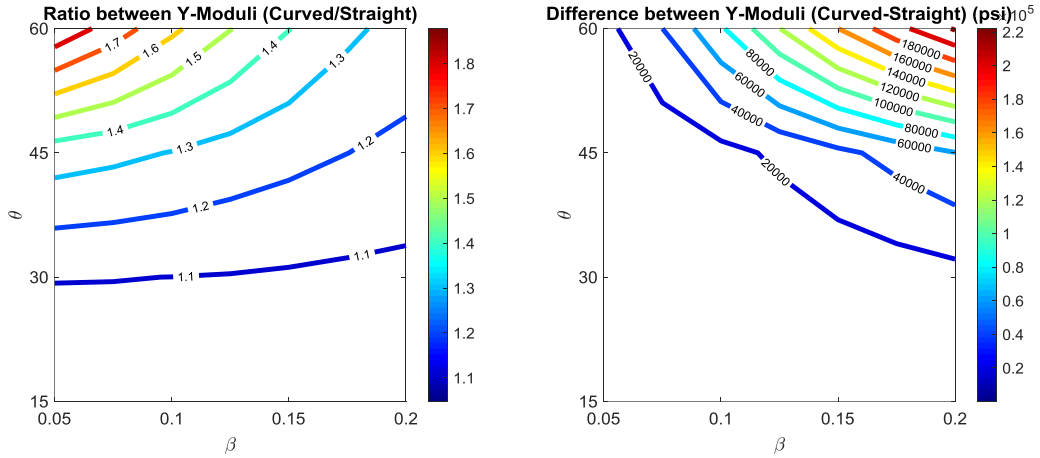

Figure 6 – Ratio and differences in y-modulus between curved- and straight- walled cells

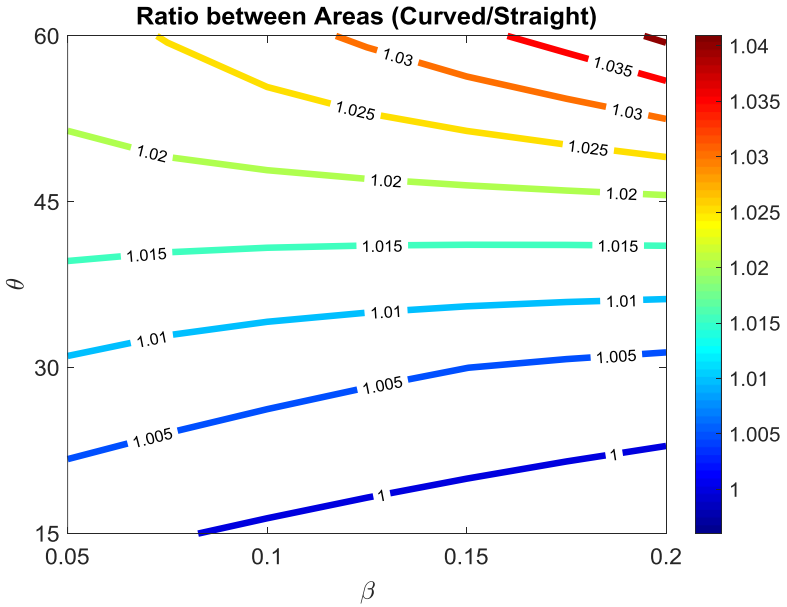

Figure 7 – Ratio between frontal area of cells with curved and straight inclined walls

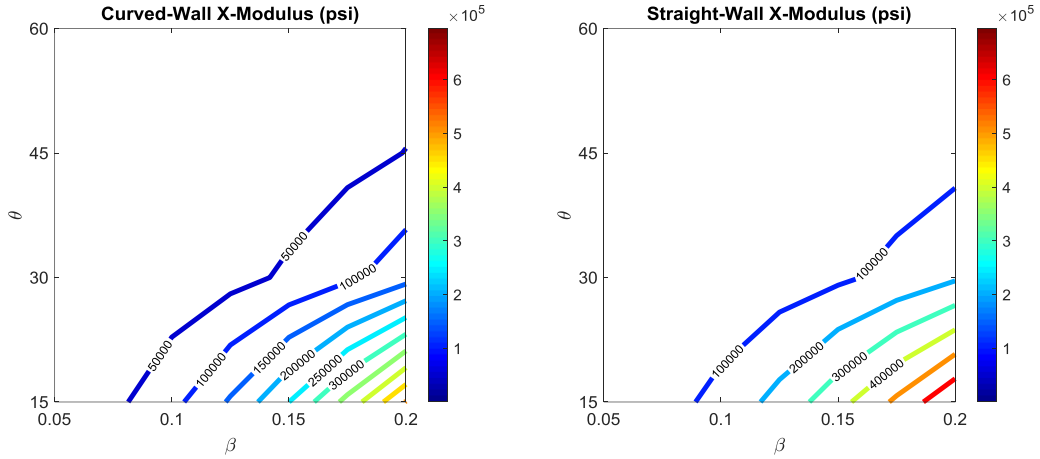

Figure 8 – System modulus for various cell geometries under x-direction loading

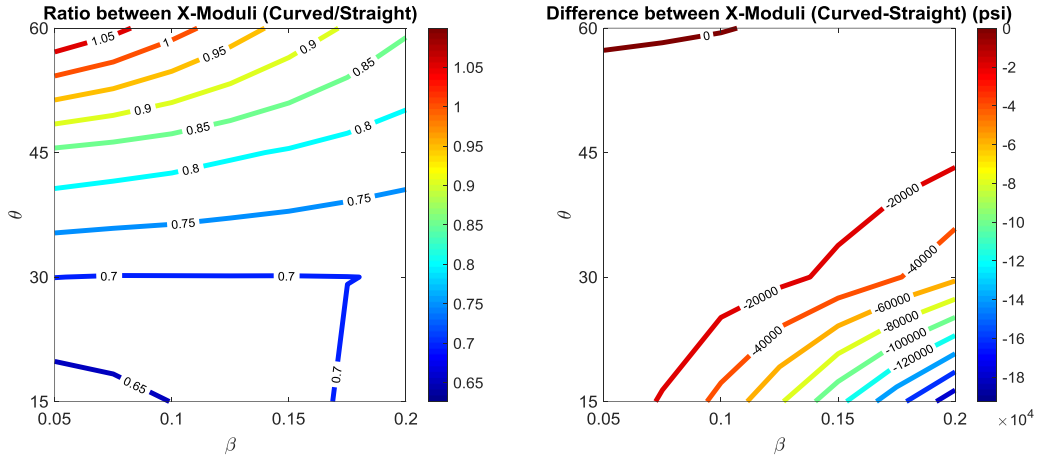

Figure 9 – Ratio and differences between x-modulus between curved- and straight- walled cells

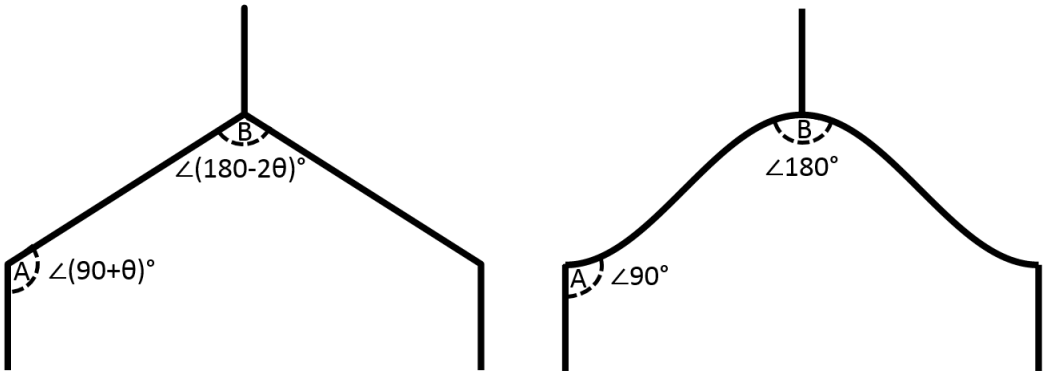

Figure 10 – Comparison of junction angles for straight- and curved-wall lattices

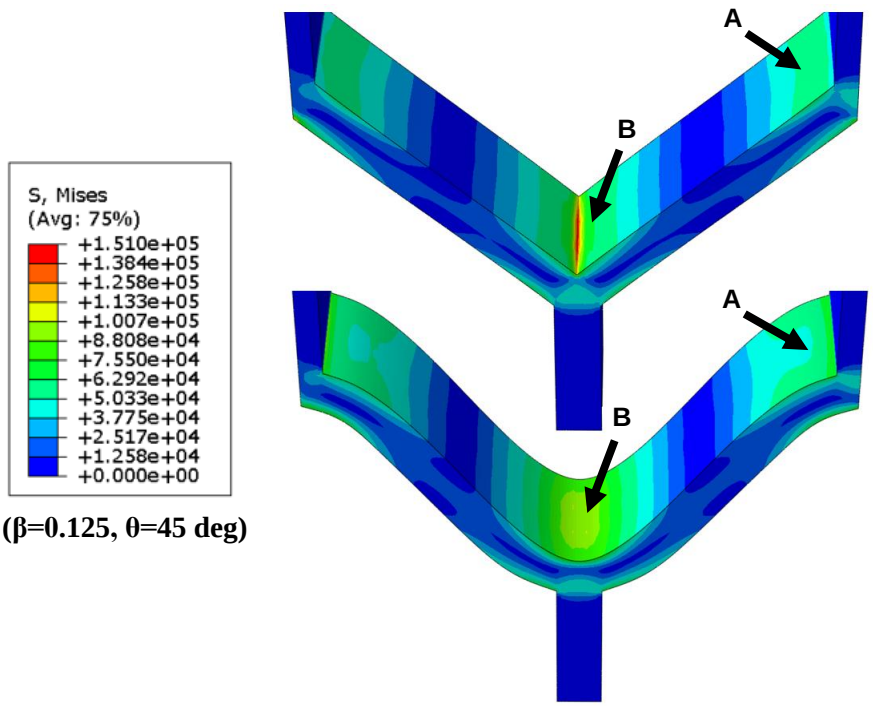

(β=0.125, θ=45 deg)

Figure 11a – Von Mises stress for straight- and curved-wall cells in x-direction loading

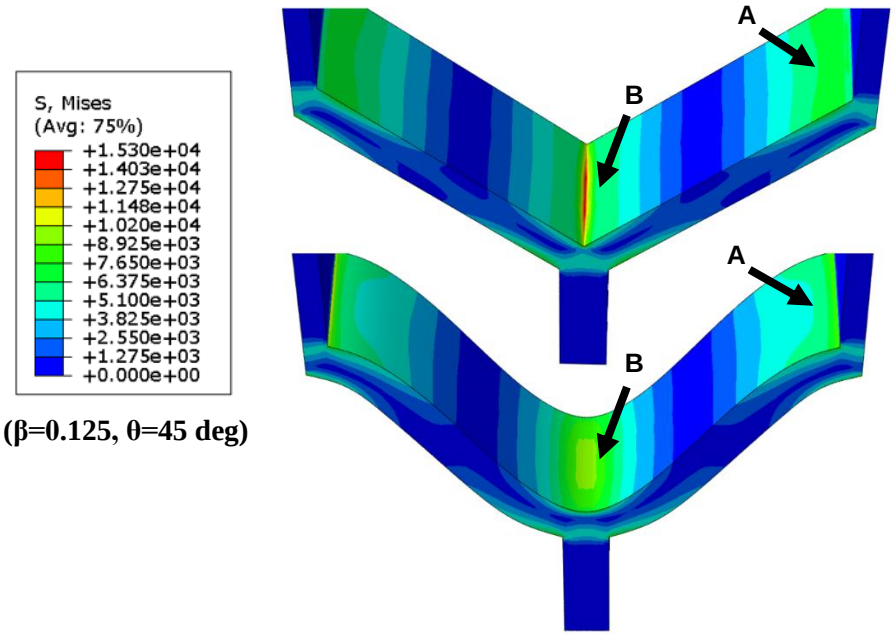

(β=0.125, θ=45 deg)

Figure 11b – Von Mises stress for straight- and curved-wall cells in y-direction loading

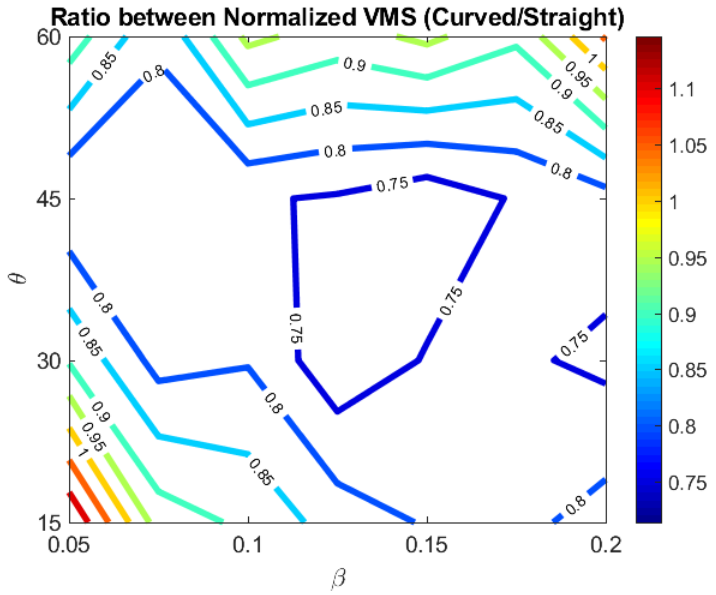

Figure 12 – Ratio between normalized Von Mises stress for curved- and straight-wall cells in x-direction loading

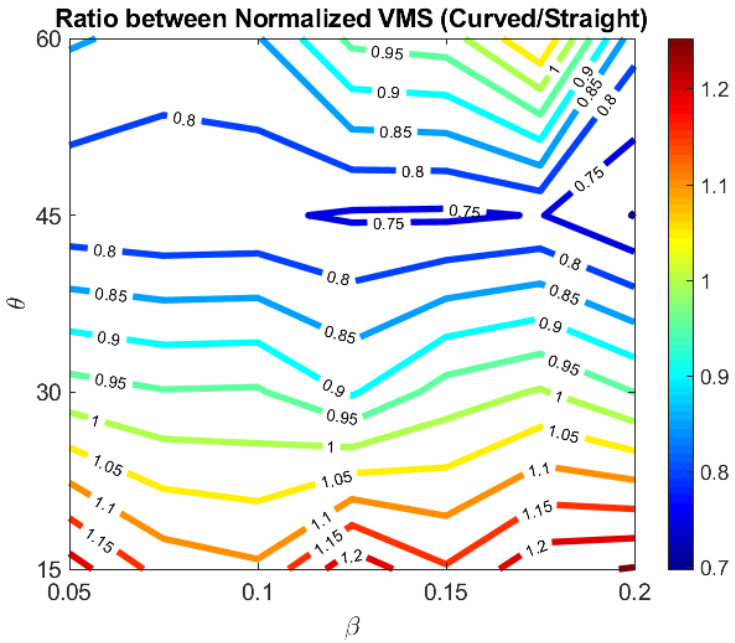

Figure 13 – Ratio between normalized Von Mises stress for curved- and straight-wall cells in y-direction loading

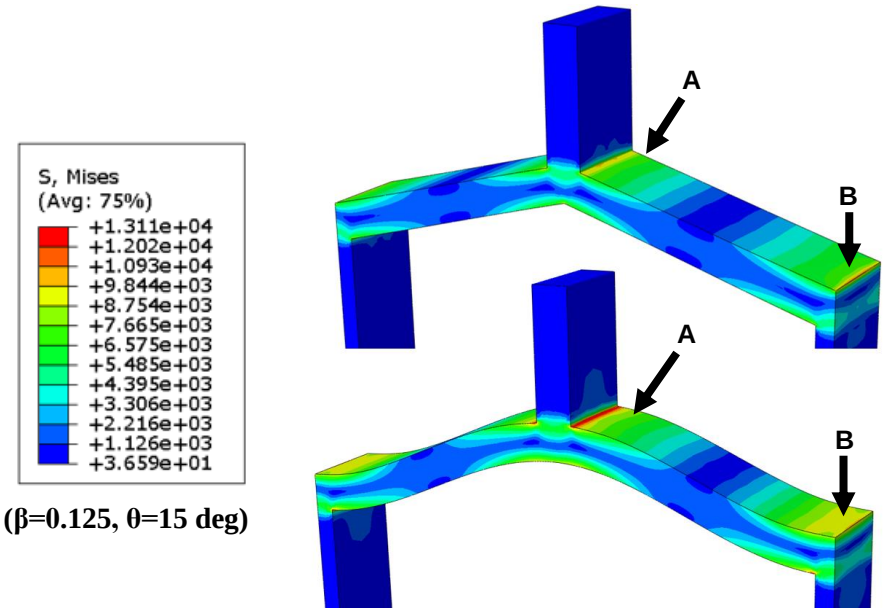

(β=0.125, θ=15 deg)

Figure 14 – Von Mises stress for straight- and curved-wall cells in y-direction loading

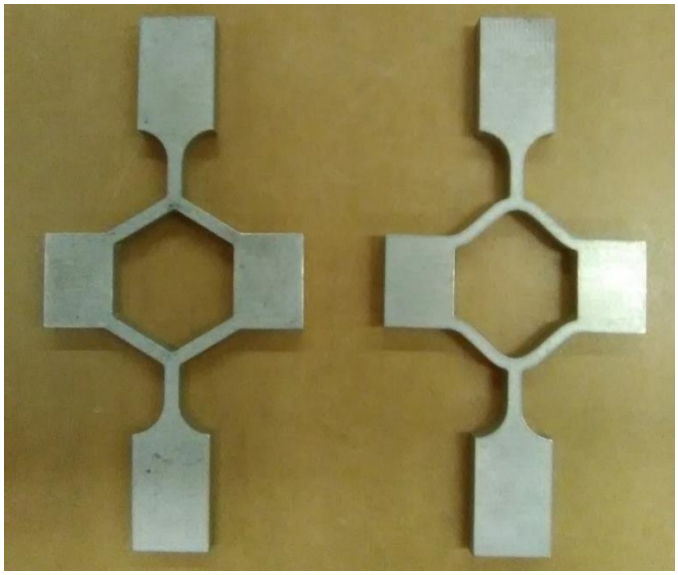

Figure 15 – Straight- and curved-wall cells waterjet cut from Aluminum

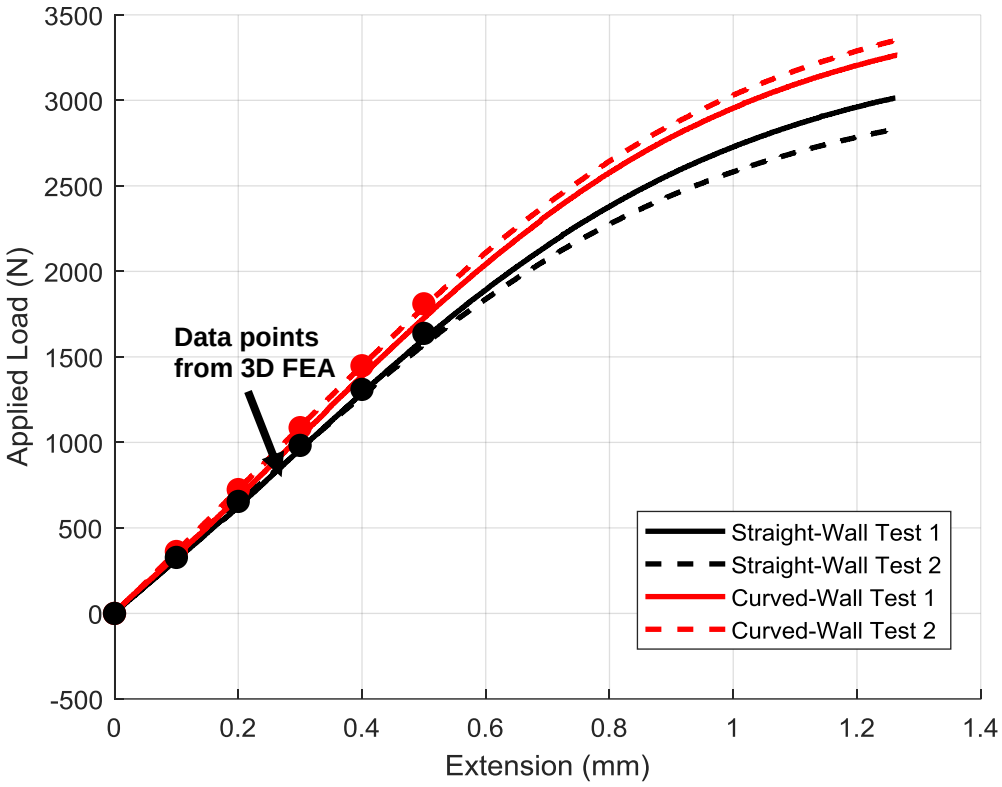

Figure 16 – Load versus displacement curve for tensile samples

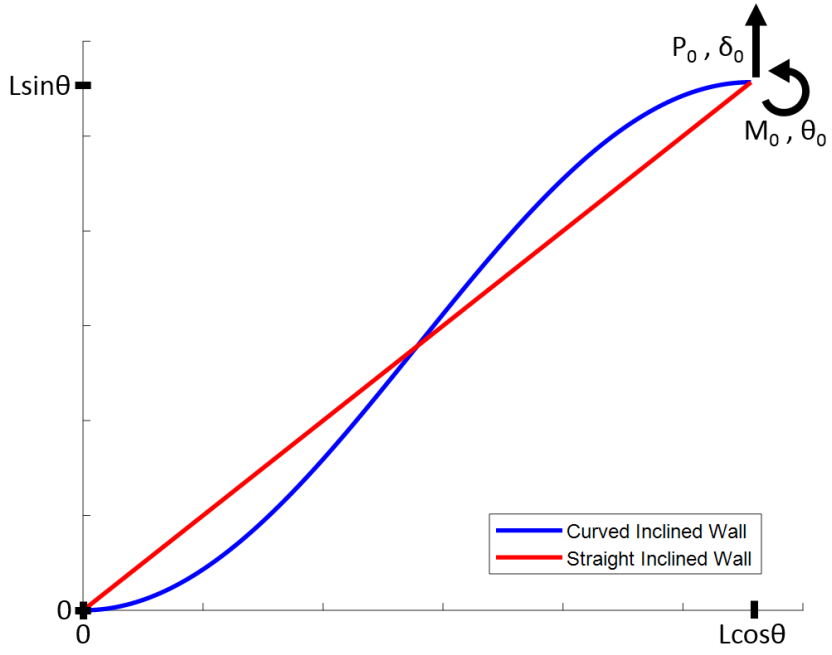

Figure 17 – Reduced system for energy-based analytical solution

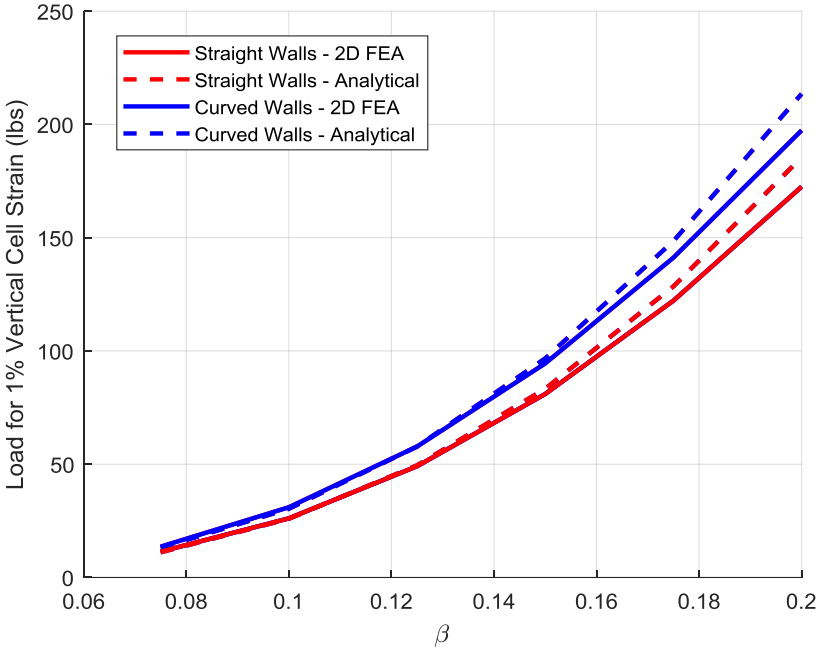

Figure 18 – Comparison between 2D FEA and simplified analytical solution

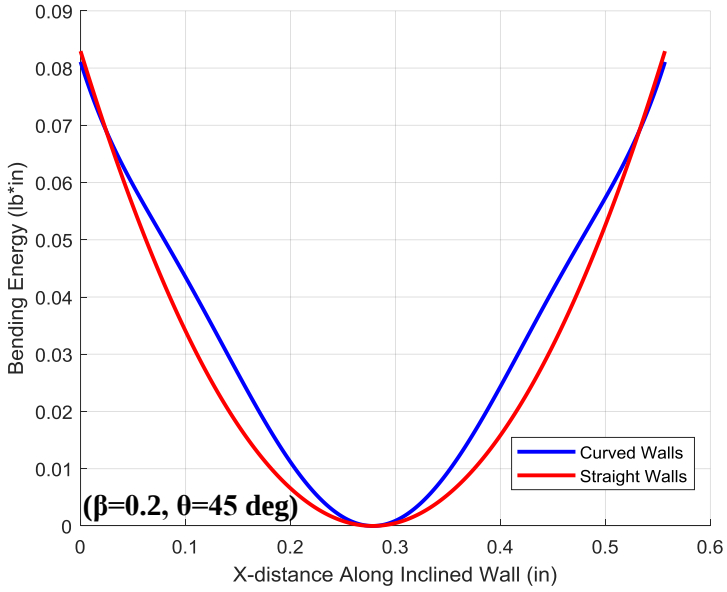

Figure 19 – Bending energy distribution for straight- and curved-wall cells under 1% strain in the y-direction

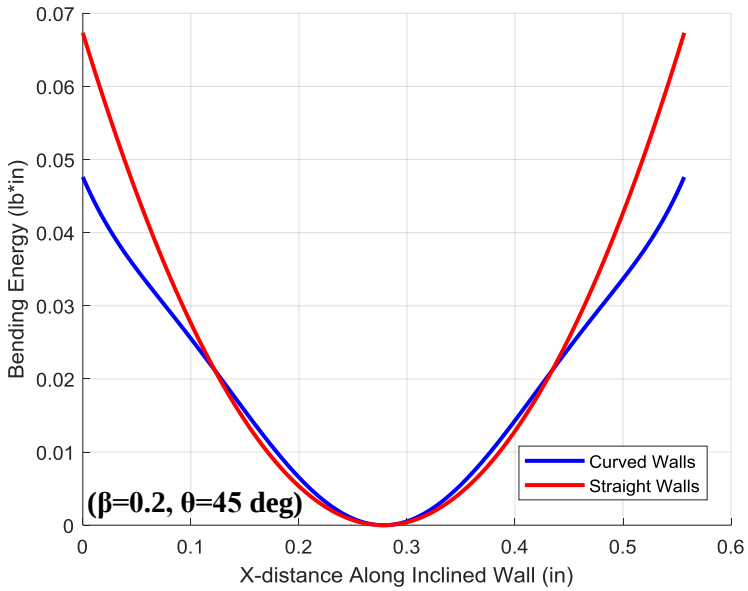

Figure 20 – Bending energy distribution for straight- and curved-wall cells under 10 lbs load in the y-direction

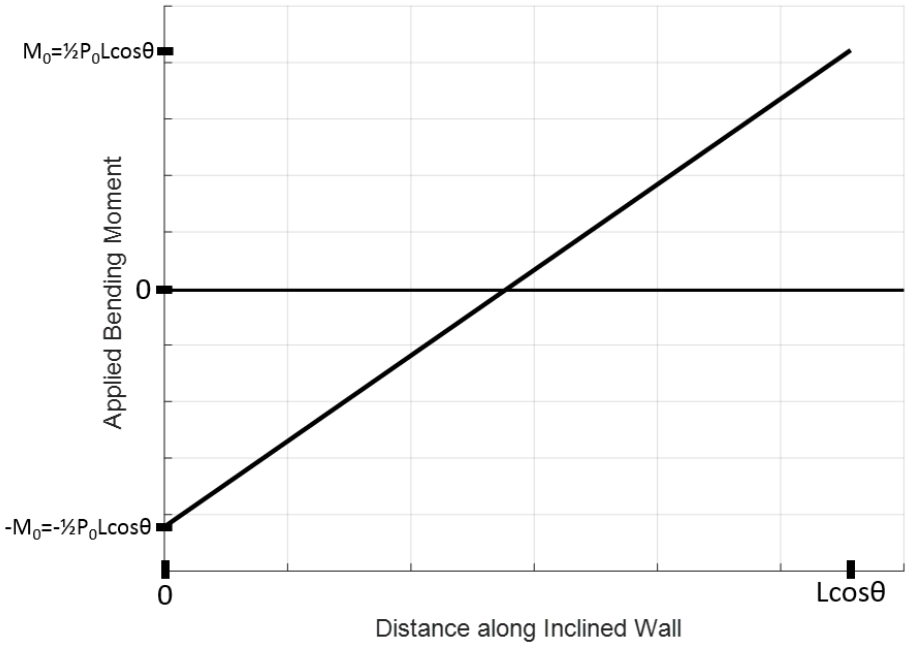

Figure 21 – Bending moment along inclined wall length